Acta Crystallographica Section B
Structural Science
ISSN 0108-7681

High-pressure crystal structure of the non-linear optical compound BiB_3O_6 from two-dimensional powder diffraction data

R. E. Dinnebier,[a]* B. Hinrichsen,[b] A. Lennie[c] and M. Jansen[a]

[a]Max-Planck Institute for Solid State Research, Heisenbergstrasse 1, D-70569 Stuttgart, Germany, [b]Bruker AXS GmbH, Östliche Rheinbrückenstrasse 49, 76187 Karlsruhe, Germany, and [c]Structural and Environmental Chemistry College, Daresbury Laboratory, STFC (Science and Technology Facilities Council), Keckwick Lane, Warrington WA4 4AD, England

Correspondence e-mail: r.dinnebier@fkf.mpg.de

Received 17 June 2008
Accepted 12 September 2008

Our recently proposed method for automatic detection, calibration and evaluation of Debye–Scherrer ellipses using pattern-recognition techniques and advanced signal filtering was applied to the two-dimensional powder diffraction data of the non-ferroelectric, non-centrosymmetric non-linear optical (NLO) compound α-BiB_3O_6 as a function of pressure. At ambient conditions, α-BiB_3O_6 crystallizes in the space group *C*2 (phase I). In the pressure range between P = 6.09 and 6.86 GPa, it exhibits a first-order phase transition into a structure with the space group *C*1 (*P*1) [phase II at P = 8.34 GPa: a = 7.4781 (6), b = 3.9340 (4), c = 6.2321 (6) Å, α = 93.73 (1), β = 102.93 (1), γ = 90.76 (1)°, and V = 178.24 (3) Å^3]. Non-linear compression behaviour over the entire pressure range is observed, which can be described by two Vinet relations in the ranges from P = 0.0 to 6.09 GPa, and from P = 6.86 to 11.6 GPa. The extrapolated bulk moduli of the high-pressure phases were determined to be K_0 = 38 (1) GPa for phase I, and K_0 = 114 (10) GPa for phase II. The crystal structures of both phases were refined against X-ray powder diffraction data measured at several pressures between 0.0 and 11.6 GPa. The structural phase transition of α-BiB_3O_6 is mainly characterized by a reorientation of the $[BO_3]^{3-}$ triangles, the $[BO_4]^{5-}$ tetrahedra and the lone electron pair which is localized at Bi^{3+}, in order to optimize crystal packing.

1. Introduction

In the course of a long-term investigation of the effect of stereochemically active lone pairs on crystal structures at high pressure (Pb_3O_4: Dinnebier *et al.*, 2003; SeO_2: Orosel *et al.*, 2004; Sb_2O_4: Orosel *et al.*, 2005; $FeSb_2O_4$: Hinrichsen, Dinnebier, Rajiv *et al.*, 2006; $SnSO_4$: Hinrichsen *et al.*, 2008), α-bismuth borate was studied in the pressure range from ambient pressure to 11.6 GPa. In general, lone pairs can be viewed as pseudo-ligands in compounds exhibiting increasingly covalent bonding contributions (Gillespie, 1967; Gillespie & Robinson, 1996), significantly changing the space requirements and bonding situation in the affected solids. Due to the high polarizability of cations with 'lone pairs' and since the so-formed crystal structures are rather open, it can be expected that such compounds undergo pressure-induced phase transitions. This concept has recently been proven by analyzing the high-pressure phases of the compounds mentioned above. In the case of the mixed-valent oxide Pb_3O_4 (Dinnebier *et al.*, 2003), the 'lone pair' was forced into a quasi *s*-type state at pressures above 5.6 GPa, removing almost all anisotropies in the coordination sphere of Pb^{2+}. If such structures could be quenched, one would expect interesting electronic properties to arise with semi-conducting or even metallic behavior in the case of delocalized *s*-orbital electrons.

The crystal structure of the lone-pair bearing compound α-BiB_3O_6 has recently attracted considerable interest as a polar, non-ferroelectric compound with exceptional nonlinear optical (NLO) properties (Alexander *et al.*, 2008; Bi *et al.*, 2003; Costantinos *et al.*, 2005; Ghotbi & Ebrahim-Zadeh, 2004, 2005; Ghotbi, Ebrahim-Zadeh *et al.*, 2006; Ghotbi, Esteban-Martin & Ebrahim-Zadeh, 2006; Hartke *et al.*, 2007; Hellwig *et al.*, 1998, 2000; Jang *et al.*, 2008; Masood *et al.*, 2004, 2006*a*,*b*, 2007; Masood & Majid, 2005*a*,*b*; Peltz *et al.*, 2005*a*,*b*; Petrov *et al.*, 2007; Ruseva & Hald, 2004; Sun, Ghotbi, Minardi & Ebrahim-Zadeh, 2007; Sun, Ghotbi & Ebrahim-Zadeh, 2007; Teng *et al.*, 2001; Tzankov & Petrov, 2005; Umemura *et al.*, 2007; Valentin *et al.*, 2007; Häussermann *et al.*, 2001). A technical application is possible, since single crystals of sufficient size and quality could be synthesized (Becker *et al.*, 1999; Teng *et al.*, 2001). The crystal structure of α-BiB_3O_6 at ambient conditions can be described as a phylloborate layer structure consisting of alternating layers of borate anions and bismuth cations perpendicular to the c^* axis (Fröhlich *et al.*, 1984; Fig. 1). The borate groups consisting of $[BO_3]^{3-}$ triangles and $[BO_4]^{5-}$ tetrahedra in a 2:1 ratio form a two-dimensional net linked by corners. The coordination of the BiO_6 polyhedron is highly irregular, due to the non-bonding lone-pair electrons of the sp^3-hybridized Bi^{3+} orbitals. The NLO properties were attributed to the bonds in the triangular $[BO_3]^{3-}$ units and to the lone pair at the Bi^{3+} cation (Hellwig *et al.*, 1998). α-BiB_3O_6

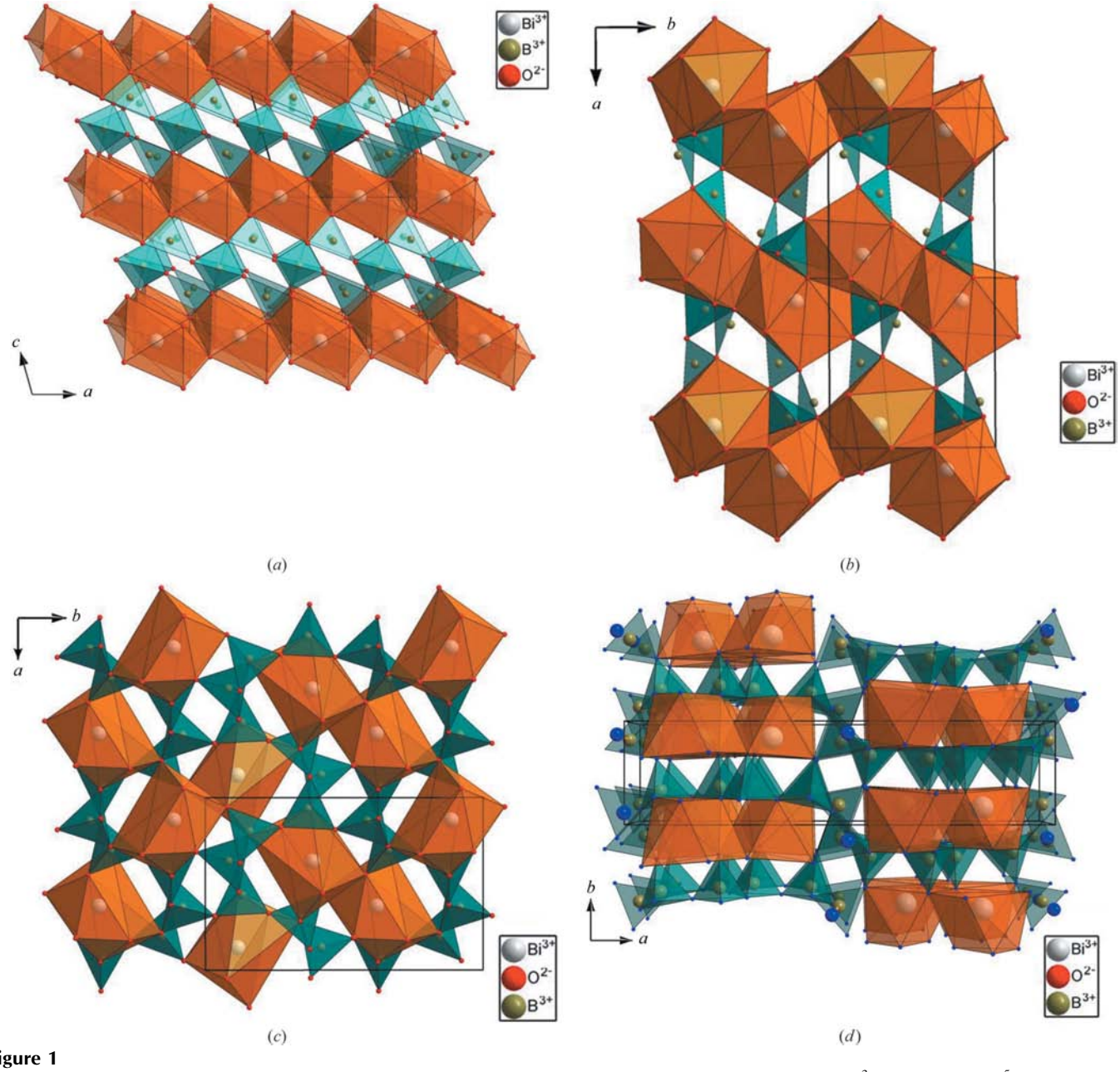

Figure 1
Perspective projections of the known crystal structures of α-, β-, γ- and δ-bismuth triborate (BiB_3O_6). The $[BO_3]^{3-}$ triangles, $[BO_4]^{5-}$ tetrahedra and BiO_x polyhedra are drawn.

exhibits one of the largest anisotropies in the elastic constants (Haussühl *et al.*, 2006) and the thermal expansion (Stein *et al.*, 2007) observed in ionic crystals, anisotropy which is attributed to the preferential orientation of the lone electron pair of Bi^{3+} (Haussühl *et al.*, 2006). In the temperature range from 8 to 999 K, no structural phase transition was found for α-BiB_3O_6. Preliminary investigations using Raman spectroscopy at room temperature and elevated pressure did not show any evidence for structural changes up to a pressure of $p = 18$ GPa (Hellwig, 2002).

Recently, three additional polymorphs of BiB_3O_6 have been found, two of which (β-, and γ-BiB_3O_6) exhibit a centre of symmetry (and thus no NLO properties) in the space group $P2_1/n$ (Li *et al.*, 2005), while the third one (δ-BiB_3O_6) crystallizes in the non-centrosymmetric space group $Pna2_1$ (Knyrim *et al.*, 2006; Fig. 1).

Because of the high compressibility due to the lone pair of the Bi^{3+} cation and the extreme anisotropy of the thermal expansion, we decided to investigate the pressure dependence of the crystal structure of α-BiB_3O_6, a study which we consider a prerequisite for future investigations of additional possibly quenchable high-pressure modifications. For this purpose, *in situ* X-ray powder diffraction measurements were performed at room temperature and elevated pressures, using a diamond–anvil cell (DAC).

High-pressure powder diffraction data from DACs are often difficult to interpret due to the fact that usually very few extremely intense spikes, originating from grains in an ideal diffraction position, tend to dominate the diffraction pattern. A recently developed phenomenological model for the description of such intensity distributions turned out to be extremely helpful in extracting reliable peak intensities out of the powder patterns of α-BiB_3O_6 at high pressure by automatic determination of optimized fractile filters (Hinrichsen *et al.*, 2007).

2. Experimental

2.1. Synthesis and X-ray diffraction measurements

A highly pure sample of α-BiB_3O_6 was received from Petra Becker, University of Cologne. The starting substance was analyzed using laboratory X-ray powder diffraction and was found to contain no detectable impurities.

High-pressure powder diffraction experiments were performed at the high-flux powder diffraction Station 9.5HPT

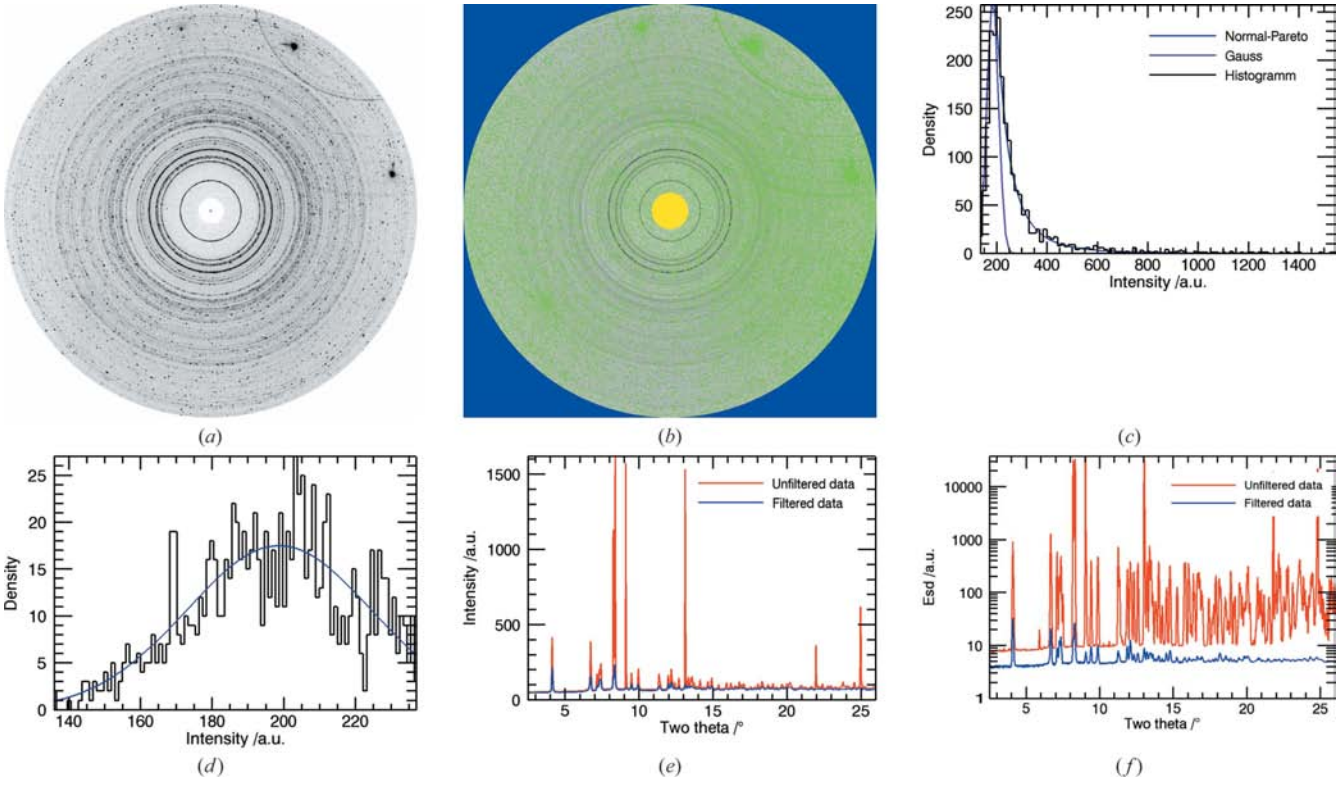

Figure 2
Powder diffraction data of ϵ-BiB_3O_4 at $P = 8.35$ GPa, collected by a two-dimensional image-plate detector. The raw image (*a*) and the filtered image (*b*) are shown. The green mask represents the pixels which belong to the top 48% of the intensities per integration bin. The blue mask shows the pixels which belong to the bottom 2% of the intensities per integration bin. The yellow mask is the beam stop mask filtering the first 2° 2θ of the diffraction image. Only the uncoloured region of the image is used for the integration to a one-dimensional diffractogram. The intensity distribution of an unfiltered (*c*) and filtered (*d*) bin are displayed showing fits to the expected normal and the proposed normal-Pareto distributions. The effect of filtering is further visualized on the final integrated and background corrected pattern (*e*) and on the standard deviations (*f*) (in red the integrated pattern of the unfiltered image, in blue the diffractogram of the filtered image).

of Daresbury Laboratory, England, situated 30 m from the 5 T superconducting wavelength shifter. A wavelength of 27.93 keV (0.44397 Å) was selected by scanning a Si(111) reflection from a bent silicon crystal in Laue geometry over the absorption edge of an indium foil. The focused monochromatic beam was further reduced by a Pt disc pinhole of 70 µm diameter (Lennie *et al.*, 2007). The sample was hand ground in an agate mortar for ∼ 20 min. A small amount of sample was loaded in a symmetric Merrill–Bassett-type diamond–anvil cell (DAC). Silicone oil was used as a pressure medium (Shen *et al.*, 2004). No rotation during the exposure was performed. The pressure was measured off-line by the ruby line shift method (Forman *et al.*, 1972; Mao *et al.*, 1982). The diffraction patterns were recorded by a marresearch mar345 online image-plate system. Two datasets with a total of 19 images at pressures ranging from P = 0.0 to 11.6 GPa were recorded. Exposure times ranged from 300 to 420 s, depending on the detector saturation.

2.2. Data reduction and structure determination

The image-plate orientation and sample-to-plate distance were determined using a silicon powder standard (NIST 640b). Initially, a traditional calibration routine was run using the Powder3D IP software (Hinrichsen *et al.*, 2006). The results were later refined using the whole image refinement (WIR) procedure (Hinrichsen *et al.*, 2006). To do this successfully the background had to be determined and the outlier intensities had to be extensively filtered prior to the refinement.

The image-plate recordings of α-BiB_3O_6 at high pressure were quite spotty (Fig. 2*a*) for reasons explained in the introduction and needed effective filtering before integration to extract the underlying information correctly. A fractile filter removing a fraction of the highest and lowest intensities from each bin was used. The fraction to be removed was determined using the relation of the normal to the normal-Pareto distributed intensities of a strong peak (Hinrichsen *et al.*, 2007). This resulted in 58% of the highest intensity being removed from each bin before integration (Fig. 2*b*). This filtering method led to approximately normally distributed intensities, ideally suited for least-squares refinement (Figs. 2*c* and *d*). Integration of all datasets was then performed with Powder3D IP, resulting in 19 diagrams of corrected intensities *versus* the scattering angle 2θ (Fig. 3). Following successful data reduction, the scattering profile gave evidence of a phase transition around P = 6.5 GPa. We name the new high-pressure phase ϵ-BiB_3O_6.

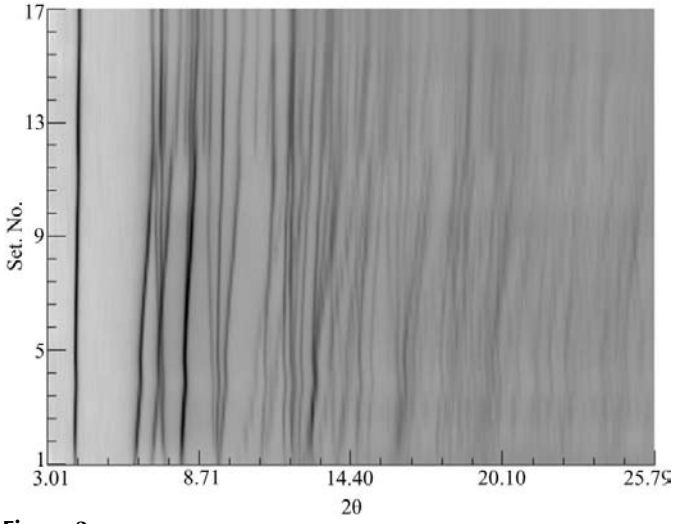

Figure 3
A simulated Guinier plot of α-BiB_3O_6 in the pressure range from 0.0 up to 12 GPa, showing the progression of the intensity normalized powder pattern over the measured (nonlinear) pressure range. The strong anisotropy of the pressure dependency of the Bragg reflections is clearly visible.

Table 1
Lattice parameters and details of the refinements of α-BiB_3O_6 at P = 4.3 GPa and ϵ-BiB_3O_6 at P = 8.34 GPa.

R_p, R_{wp} and $R(F^2)$ refer to the Rietveld criteria of fit for the profile, weighted profile and integrated intensities, respectively, defined in the *TOPAS* software.

Phase	α-BiB_3O_6	ϵ-BiB_3O_6
Pressure (GPa)	4.3	8.34
a (Å)	7.3786 (5)	7.4781 (6)
b (Å)	4.3992 (3)	3.9340 (4)
c (Å)	6.3388 (5)	6.232 1(6)
α (°)	90	93.73 (1)
β (°)	104.374 (5)	102.93 (1)
γ (°)	90	90.76 (1)
V (Å^3)	199.31 (2)	178.24 (3)
V/Z (Å^3)	99.66	89.12
Z	2	2
Space group	$C2$	$C1$ ($P1$)
ρ_{calc} (g cm^{-3})	5.622	6.287
Formula weight (g mol^{-1})	674.82	674.82
μ (cm^{-1})	125.7	140.5
Temperature (K)	293	293
R_p	0.0193	0.0158
R_{wp}	0.0279	0.0218
$R(F^2)$	0.0140	0.0110
No. of reflections	137	206
No. of variables	37	69
No. of refined atoms	7	10
Wavelength (Å)	0.44397	0.44397
2θ range (°)	3–26	3–26
Step size (° 2θ) (after rebinning)	0.01	0.01

Using the published structural data of the ambient pressure phase as starting parameters (Donaldson & Puxley, 1972), the powder diffraction patterns of α-BiB_3O_6 at increasing pressure were subjected to consecutive Rietveld refinements using the program *TOPAS*, version 4.0 (Bruker AXS, 2007; Coelho, 2004).

The first 12 patterns showed excellent convergence using the starting model. Starting with the 13th powder pattern at P = 6.86 GPa no convergence could be reached. All attempts to find a set of unit-cell parameters using conventional indexing algorithms failed. From the observation that the angular positions of the main reflections do not change much during the phase transition and that no additional lines at low angle occur, similar unit-cell parameters and volumes were expected for ϵ-BiB_3O_6. A recently developed indexing algo-

rithm called LP-search (Bruker AXS, 2007), which is independent of *d*-spacing extraction, was used to index the powder pattern of the high-pressure phase of ϵ-BiB_3O_6. LP-search minimizes on a figure-of-merit function that gives a measure of correctness for a particular set of lattice parameters, for which lower and upper bounds need to be specified. A triclinic B-centred unit cell (which was later transformed to its C-centred analogue), quickly led to an acceptable agreement with respect to the experimental data. The number of formula units per unit cell could be determined to be $Z = 2$ from volume increments. The extinctions found in the powder patterns clearly indicated $C1$ or $C\bar{1}$ as possible space groups, of which $C1$ could later be confirmed by Rietveld refinement (Rietveld, 1969). Structure determination and refinement was performed for the dataset at a pressure of $P = 8.34$ GPa using the program *TOPAS*. The peak profiles and precise lattice parameters were determined by a LeBail fit (Le Bail *et al.*, 1988) using *TOPAS*. A simulated annealing (SA) run (Coelho, 2000) using a merging radius of 0.6 Å immediately found the atomic positions for the Bi atom and some candidates for O atoms. Because of the high scattering contrast between Bi atoms and O and B atoms, no positions for the B and O atoms could be confirmed with confidence. To stabilize the SA run, a simple anti-bumping penalty function in the form of a Lennard–Jones (12-6) potential was introduced, avoiding close contacts between the atoms. The crystal structure could thus be completely solved, confirming two triangular and one tetrahedral environment for the three crystallographically distinct B atoms. To verify the solution, an independent structure determination was performed using the program *Endeavour* (Crystal Impact, 2008) which combines global optimization of the difference between the calculated and measured diffraction pattern and of the potential energy of the system. Except for the origin of the unit cell, an identical solution was obtained, giving confidence in the correctness of the crystal structure. Due to relatively shallow minima at the positions of the light elements (resulting in relatively large variations of the atomic positons) slack soft constraints for all B—O distances and planarity constraints for the two triangular BO_3 groups were introduced for the following Rietveld refinement, which converged to a Bragg R value of 0.010. Three small Bragg reflections of the gasket material were included in the refinement as single peaks; agreement factors (R

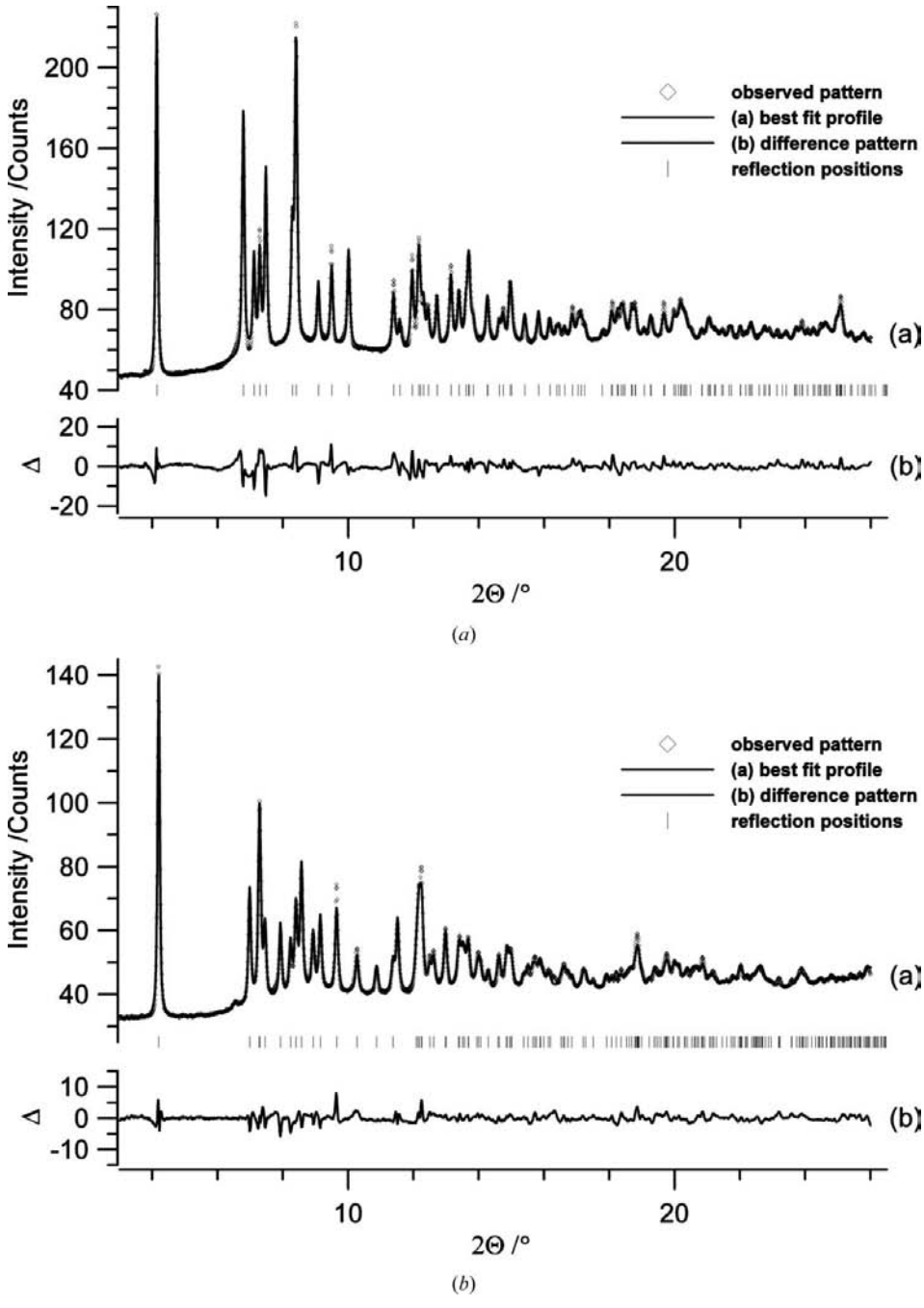

Figure 4
The Rietveld refinement plot of the monoclinic α-phase of BiB_3O_6 at $P = 4.3$ GPa (*a*) and the triclinic ϵ-phase of BiB_3O_6 at $P = 8.34$ GPa (*b*) showing the experimental data as open circles, the calculated pattern as the upper solid line and the difference pattern (same scale as powder pattern) as the lower solid line. The positions of the reflections are marked by vertical lines.

Table 2
Selection of bond lengths (Å) and angles (°) of α-BiB_3O_6 at P = 4.3 GPa and ϵ-BiB_3O_6 at P = 8.34 GPa.

	α-BiB_3O_6	ϵ-BiB_3O_6
Bi—O	2.091 (7) 2×	2.06 (2)
	2.385 (6) 2×	2.12 (1)
	2.509 (8) 2×	2.50 (1)
		2.54 (1)
		2.55 (1)
		2.58 (2)
		2.60 (2)
		2.60 (1)
B1—O (BO_4)	1.51 (3) ×2	1.46 (1)
	1.52 (3) ×2	1.47 (2)
		1.51 (2)
		1.55 (1)
B2—O (BO_3)	1.37 (2)	1.32 (1)
	1.40 (2)	1.39 (1)
	1.47 (2)	1.48 (2)
B3—O (BO_3)	1.37 (2)	1.34 (1)
	1.40 (2)	1.35 (2)
	1.47 (2)	1.42 (2)
O—O (min)	2.29 (1)	2.28 (1)
Bi—Bi (min)	4.29 (0)	3.93 (1)
Bi—B (min)	2.99 (1)	2.71 (1)
O—Bi—O	55.8 (2)–146.8 (2)	52.4 (3)–167.7 (5)
O—B1—O (BO_4)	105 (1)–115 (1)	100 (1)–117 (1)
O—B2—O (BO_3)	108 (1)–142 (1)	107 (1)–141 (1)
O—B3—O (BO_3)	108 (1)–142 (1)	110 (1)–134 (1)

values) are listed in Table 1. The coordinates are given in the supplementary material,[1] and a selection of intra- and intermolecular distances and angles is given in Table 2. No additional symmetry could be detected using the programs *PLATON* (Spek, 2003) and *K-plot* (Hundt *et al.*, 1999).

In addition, Rietveld refinements (Fig. 4) were performed on all measured powder patterns in the pressure range $0.0 \leq P \leq 11.6$ GPa. The dependence of the unit-cell volume on pressure was plotted and fitted by two Vinet equations-of-state for the pressure ranges P = 0.0–6.09 GPa (α-BiB_3O_6) and P = 6.86–11.6 GPa (ϵ-BiB_3O_6; Fig. 5*a*) using the program *EosFit*5.2 (Angel, 2002). In addition, the highly anisotropic relative lattice parameters of α-BiB_3O_6 are plotted against pressure (Fig. 5*b*).

Crystallographic coordinates can be obtained from the Fachinformationszentrum Karlsruhe, D-76344 Eggenstein-Leopoldshafen, Germany; fax: (+49)7247-808-666; email: crysdata@fiz.karlsruhe.de on quoting the depository numbers CSD-419573 (ϵ-BiB_3O_6 at P = 8.34 GPa) and CSD-419574 (α-BiB_3O_6 at P = 4.3 GPa).

3. Results and discussion

The crystal structure of ambient α-BiB_3O_6 is highly compressible [bulk modulus of 38 (1) GPa] and stable to a pressure of at least P = 6.09 GPa. The positional parameters of α-BiB_3O_6 at elevated pressure vary only slightly from the published values at ambient conditions (Fröhlich *et al.*, 1984). α-BiB_3O_6 crystallizes in the non-centrosymmetric polar space group *C*2. The crystal structure of α-BiB_3O_6 is built of alternating layers of Bi atoms and networks of borate group networks. Two thirds of the boron atoms are trigonally coordinated and one third of the B atoms are tetrahedrally coordinated, with all four corners of each $[BO_4]^{5-}$ tetrahedron connected to separate $[BO_3]^{3-}$ triangles. All $[BO_3]^{3-}$ triangles share two corners with neighbouring $[BO_4]^{5-}$ tetrahedra with the remaining O atom bonded exclusively to two Bi^{3+} ions. The trivalent bismuth cations are irregularly coordinated by 4 + 2 O atoms, formally forming $[BiO_6]$ units sharing six edges with neighbouring $[BiO_6]$ units (Fig. 6). The effect of the lone-pair electrons on the crystal structure is quite visible through

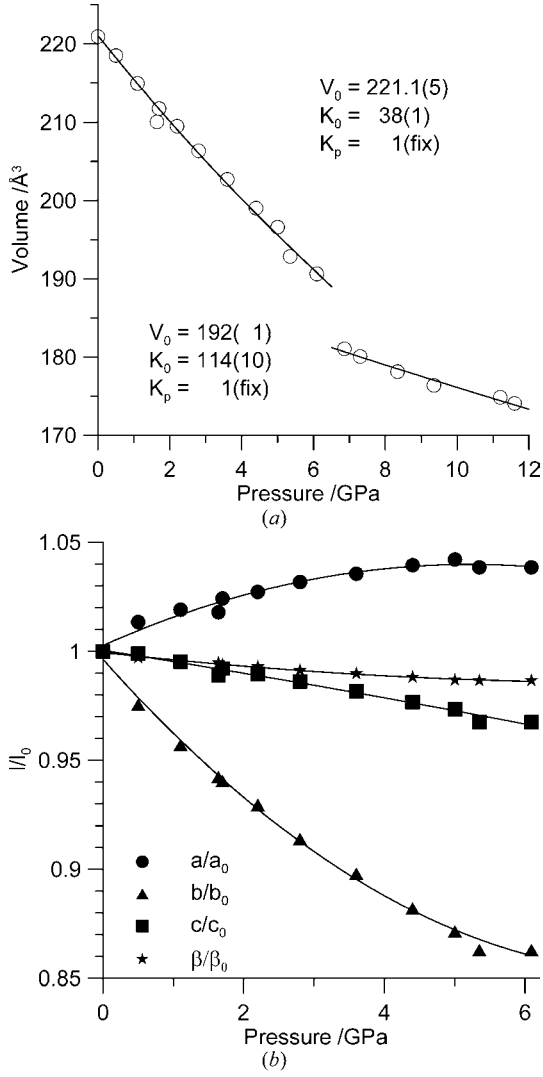

Figure 5
(*a*) The unit-cell volume of α-bismuth triborate (BiB_3O_6) is shown as a function of pressure. The solid lines are those of a Vinet equation-of-state function fitted to the data points. The bulk modulus (K_0) and volume at ambient pressure (V_0) are given. (*b*) Plot showing the progression of the relative lattice parameters of α-bismuth triborate (BiB_3O_6) in dependence on pressure over the stability range of this phase. The lines are a guide to the eyes only.

[1] Supplementary data for this paper are available from the IUCr electronic archives (Reference: KD5025). Services for accessing these data are described at the back of the journal.

open channels down the c^* axis. The largest convexity of the channels is along the b axis, which is exactly the direction in which the soft lone-pair electrons of Bi^{3+} point (Fig. 7). The channels are reminiscent of those in the AB_2O_4-type structures in which the lone pairs of B atoms cause large channels running through the structure (Dinnebier *et al.*, 2003; Hinrichsen, Dinnebier, Rajiv *et al.*, 2006). The main effect of increasing external pressure on the crystal structure of α-BiB_3O_6 is a strong anisotropic compression of the unit cell (Fig. 5) with the maximum compression along the b axis due to the soft lone pairs of Bi^{3+} (Fig. 7). Interestingly, the a axis expands with increasing pressure over the entire range of existence of α-BiB_3O_6. Haussühl *et al.* (2006), who derived the full elastic tensor from ultrasonic measurments on single crystals and Stein *et al.* (2007), who measured the thermal expansion of α-BiB_3O_6, have given a detailed interpretation of the highly anisotropic behaviour of α-BiB_3O_6. Concerning the unusual expansion of the a axis with decreasing temperature/increasing pressure, both come to the conclusion that the preferential orientation of the lone electron pair of Bi^{3+} is responsible for a so-called 'Nuremberg scissor' effect within the ab plane.

Between a pressure of P = 6.09 and 6.86 GPa, α-BiB_3O_6 exhibits a first-order phase transition into a considerably stiffer [bulk modulus B = 114 (10) GPa] high-pressure phase, called ϵ-BiB_3O_6. (Fig. 5). On first impression, the crystal structure of the high-pressure ϵ phase of BiB_3O_6 is quite similar to that of α-BiB_3O_6. On closer inspection, differences can be seen in the small reorientations of the $[BO_3]^{3-}$ triangles and $[BO_4]^{5-}$ tetrahedra, and in the higher coordination of the Bi^{3+} cation. The trivalent bismuth cations are now irregularly coordinated by 2 + 6 O atoms, formally forming $[BiO_8]$ polyhedra (Fig. 6; Table 2). The Bi—O separation in two short and four (α-BiB_3O_6) or six (ϵ-BiB_3O_6) longer bonds suggest the existence of groups and thus the presence of the lone pair for the entire pressure range under investigation.

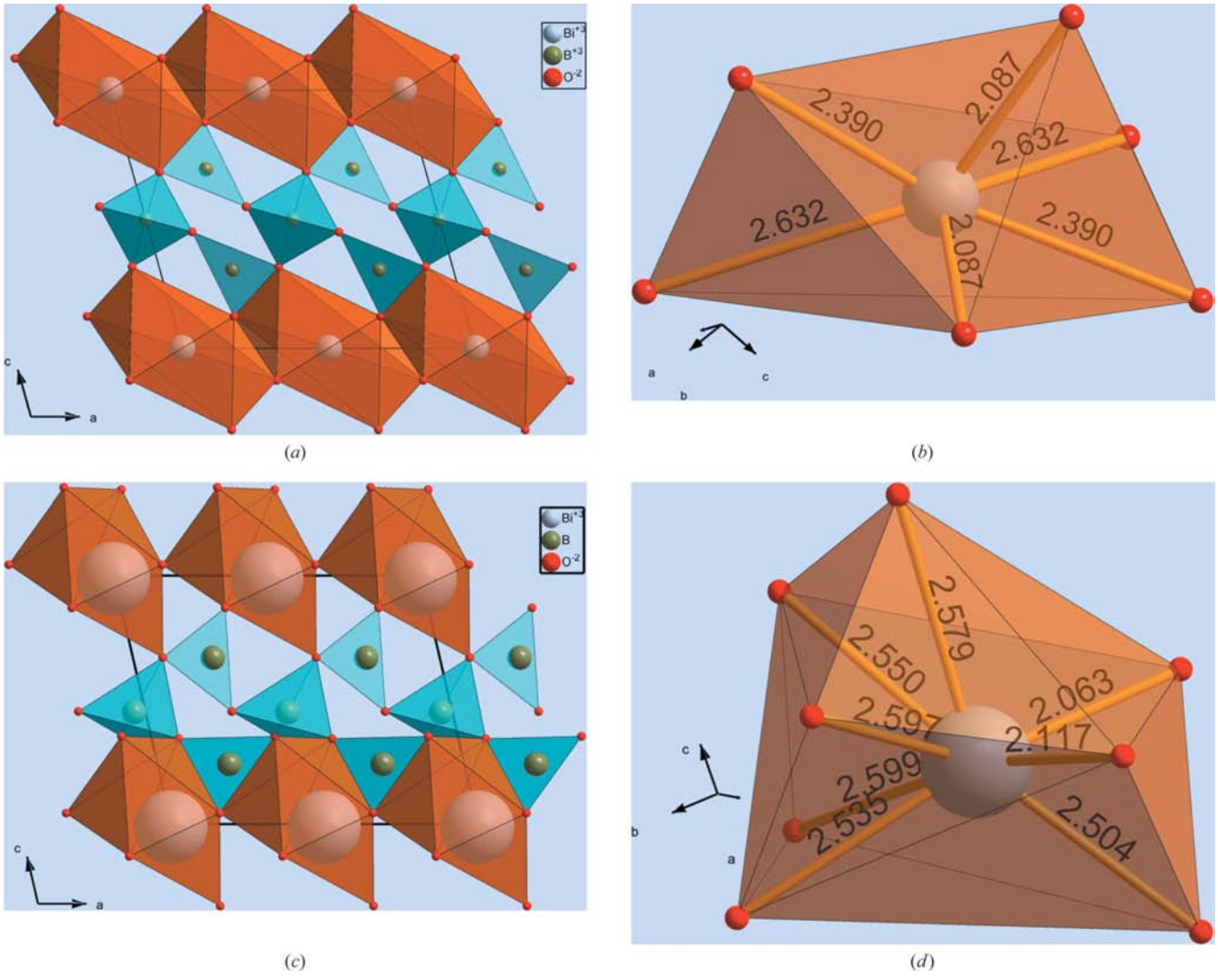

Figure 6
Projection of the crystal structure of (*a*) α BiB_3O_6 at P = 0.0 GPa and (*b*) ϵ-BiB_3O_6 at P = 8.34 GPa in similar projections. The $[BO_3]^{3-}$ triangles, $[BO_4]^{5-}$ tetrahedra and BiO_x polyhedra are drawn. In addition, the BiO_6 polyhedron of α-BiB_3O_6 and the $BiBO_8$ polyhedron of ϵ-BiB_3O_6 are drawn showing the Bi—O bond distances in Å.

Individual B—O bond distances should not be discussed as the high-scattering contrast in BiB_3O_6 does not allow a tenable analysis beyond the identification of the polyanionic structure.

From the observation that the direction of highest compressibility is along the twofold axis (*b* direction) for α-BiB_3O_6, the mechanism of the phase transition at high pressure can be understood. If the pressure is high enough, the space requirement of the electron lone pair can no longer be satisfied, and it can either be forced to adopt spherical *s*-character or evade the pressure by changing its orientation, of which the latter is responsible for the α to ϵ phase transition (Fig. 7). Both possibilities presumably would lead to a first-order phase transition.

As is the case for Pb_3O_4 (Dinnebier *et al.*, 2003), the ϵ-BiB_3O_6 phase cannot be quenched at the pressure–temperature conditions of this experiment. After pressure release, α-BiB_3O_6 is recovered.

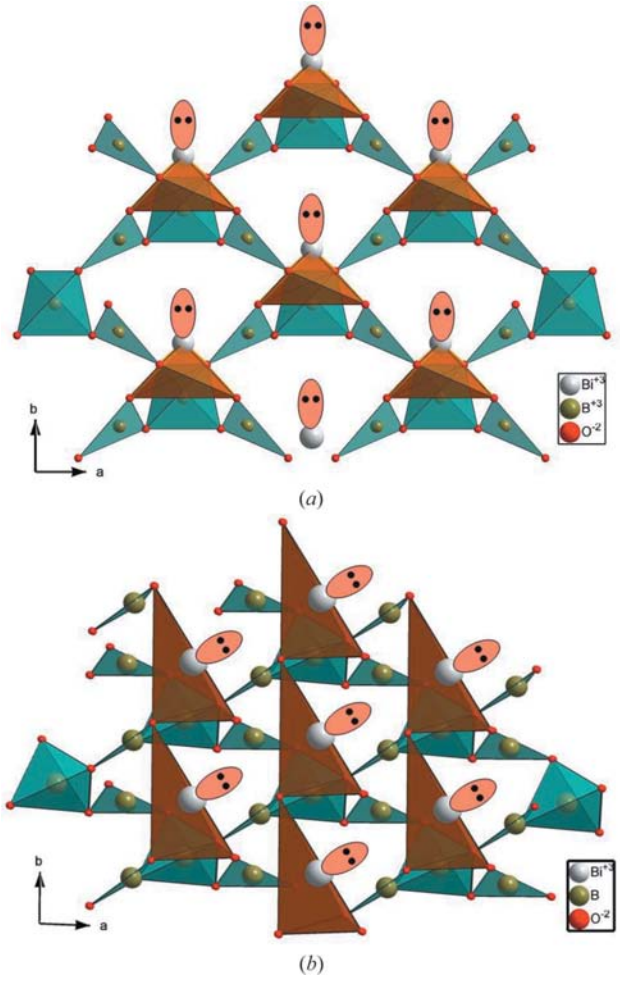

Figure 7
Crystal structures of (*a*) α- and (*b*) ϵ-bismuth triborate (BiB_3O_6) in projections showing the orientation of the free lone pair of Bi^{3+}, symbolized by an ellipse. The BO_4 tetrahedra and BO_3 triangles are drawn in blue, the BO_x polyhedra, showing only real chemical Bi—O bonds, are drawn in red.

Applying the formula of Voigt (Voigt, 1929; Hill, 1952) for polycrystalline material to the experimentally derived elastic constants at ambient conditions (Haussühl *et al.*, 2006), the bulk modulus of α-BiB_3O_6 calculates as 79 GPa, which is different from the experimentally derived bulk modulus of α-BiB_3O_6 using *in situ* powder diffraction at high pressure (38 GPa). A possible explanation could be non-hydrostatic conditions within the DAC. It is worth noting that the value of 79 GPa is close to the average of the experimentally determined bulk moduli of the α and the ϵ phase of BiB_3O_6 (76 GPa).

A comparison of the volume per formula unit of the different polymorphs of BiB_3O_6 (α = 111.3, β = 103.5, γ = 90.7, δ = 87.9, ϵ = 90.5 Å^3 at P = 6.86 GPa) reveals that the values for the γ, δ and the ϵ phases of BiB_3O_6 are very similar, suggesting that different crystal packings can exist at high pressure. While δ-BiB_3O_6 is a quenched high-pressure modification of bismuth borate synthesized in a multi-anvil apparatus at T = 1093 K and P = 5.5 GPa (Knyrim *et al.*, 2006), γ-BiB_3O_6 was prepared hydrothermally in a Teflon autoclave (Li *et al.*, 2005). In contrast to the layered crystal structures of α-, β- and ϵ-BiB_3O_6, γ- and δ-BiB_3O_6 contain three-dimensional borate frameworks, built exclusively out of corner-sharing BO_4 tetrahedra (Fig. 1). The bismuth cations are coordinated by five (γ-BiB_3O_6) or six (δ-BiB_3O_6) O atoms and the lone pair.

4. Conclusion

A first-order phase transition from α-BiB_3O_6 to a new non-centrosymmetric polymorph has been found *in situ* using a DAC at a pressure between P = 6.09 and 6.86 GPa. The new polymorph ϵ-BiB_3O_6 has been structurally characterized, and the mechanism of the phase transition can be explained on the basis of a reorientation of the lone-pair electron of the Bi^{3+} cation under pressure. Despite an increase in the coordination number of the Bi^{3+} cation from [BiO_{2+4}] (α-BiB_3O_6) to [BiO_{2+6}] (ϵ-BiB_3O_6), the lone pair of Bi^{3+} remains intact.

ϵ-BiB_3O_6 cannot be quenched as was originally expected. This behavior is in accordance with the observations made for Pb_3O_4 (Dinnebier *et al.*, 2003), $SnSO_4$ (Hinrichsen *et al.*, 2008*a*), $FeSb_2O_4$ (Hinrichsen, Dinnebier, Rajiv *et al.*, 2006), TlF and PbO (Häussermann *et al.*, 2001). Nevertheless, we are confident that the simultaneous use of high pressure and high temperature (*e.g.* laser heating or multi-anvil technique) will lead to new modifications of BiB_3O_6 with the lone-pair electrons of Bi^{3+} possibly forced into *s*-state bonding. The high-pressure phases of Sb_2O_4 (Orosel *et al.*, 2005) and SeO_2 (Orosel *et al.*, 2004) were synthesized at high pressure and high temperature and could be quenched while preserving their lone pairs.

This study shows in particular the very great importance of high-quality data and data reduction methods for extracting Rietveld quality powder diffraction patterns from two-dimensional data with extreme intensity distributions. The accuracy to determine and Rietveld-refine such a crystal structure allowing for the interpretation of minor structural

changes was made possible by employing a sophisticated newly developed algorithm for the determination of optimized intensity filters of noisy and spotty two-dimensional powder diffraction images.

Research was carried out in part at the Daresbury Synchrotron, England. Financial support by the Fonds der chemischen Industrie (FCI) and the Bundesministerium für Bildung und Forschung (BMBF) is gratefully acknowledged. Special thanks goes to Holger Putz from Crystal Impact for his help in confirming the crystal structure solution using the *Endeavour*™ program.

References

Alexander, G., Ivailo, N., Ivan, B., Frank, N. & Valentin, P. (2008). *Conference on Lasers and Electro-Optics/Quantum Electronics and Laser Science Conference and Photonic Applications Systems Technologies*, p. CFC1. Optical Society of America.

Angel, R. J. (2002). *EOSFIT*, Version 5.2. Crystallography Laboratory, Department of Geological Sciences, Virginia Tech, USA.

Becker, P., Liebertz, J. & Bohaty, L. (1999). *J. Cryst. Growth*, **203**, 149–155.

Bi, Y. *et al.* (2003). *Chin. Phys. Lett.* **20**, 1957–1959.

Bruker AXS (2007). *TOPAS*4. Bruker AXS, Karlsruhe, Germany.

Coelho, A. A. (2000). *J. Appl. Cryst.* **33**, 899–908.

Coelho, A. (2004). *TOPAS*3. Bruker AXS, Karlsruhe, Germany.

Costantinos, P., Masood, G., Abraham, S., Gholamreza, F. & Majid, E.-Z. (2005). *Conference on Lasers and Electro-Optics/Quantum Electronics and Laser Science and Photonic Applications Systems Technologies*, p. JTuC21. Optical Society of America.

Crystal Impact (2008). *Endeavour*1.5a. Crystal Impact GbR, Bonn, Germany.

Dinnebier, R. E., Carlson, S., Hanfland, M. & Jansen, M. (2003). *Am. Mineral.* **88**, 996–1002.

Donaldson, J. D. & Puxley, D. C. (1972). *Acta Cryst.* B**28**, 864–867.

Forman, R. A., Piermarini, G. J., Barnett, J. D. & Block, S. (1972). *Science*, **176**, 284–285.

Fröhlich, R., Bohatý, L. & Liebertz, J. (1984). *Acta Cryst.* C**40**, 343–344.

Ghotbi, M. & Ebrahim-Zadeh, M. (2004). *Opt. Express*, **12**, 6002–6019.

Ghotbi, M. & Ebrahim-Zadeh, M. (2005). *Opt. Lett.* **30**, 3395–3397.

Ghotbi, M., Ebrahim-Zadeh, M., Petrov, V., Tzankov, P. & Noack, F. (2006). *Opt. Express*, **14**, 10621–10626.

Ghotbi, M., Esteban-Martin, A. & Ebrahim-Zadeh, M. (2006). *Opt. Lett.* **31**, 3128–3130.

Gillespie, R. J. (1967). *Angew. Chem.* **79**, 885–896.

Gillespie, R. J. & Robinson, E. A. (1996). *Angew. Chem.* **108**, 539–560.

Hartke, R., Heumann, E., Huber, G., Kühnelt, M. & Steegmüller, U. (2007). *Appl. Phys. B*, **87**, 95–99.

Häussermann, U., Berastegui, P., Carlson, S., Haines, J. & Léger, J.-M. (2001). *Angew. Chem. Int. Ed.* **40**, 4624–4629.

Haussühl, S., Bohatý, L. & Becker, P. (2006). *Appl. Phys. A*, **82**, 495–502.

Hellwig, H. (2002). Personal communication.

Hellwig, H., Liebertz, J. & Bohaty, L. (2000). *J. Appl. Phys.* **88**, 240–244.

Hellwig, H., Liebertz, J. & Bohatý, L. (1998). *Solid State Commun.* **109**, 249–251.

Hill, R. (1952). *Proc. Phys. Soc. A*, pp. 349–354.

Hinrichsen, B., Dinnebier, R. & Jansen, M. (2008*a*). *Z. Kristallogr.* **223**, 195–203.

Hinrichsen, B., Dinnebier, R. E. & Jansen, M. (2008*b*). *Proc. EPDIC*-11, 18–2 September 2008. Warsaw, Poland.

Hinrichsen, B., Dinnebier, R. E. & Jansen, M. (2006). *EPDIC X*. Geneva.

Hinrichsen, B., Dinnebier, R. E., Rajiv, P., Hanfland, M., Grzechnik, A. & Jansen, M. (2006). *J. Phys. Condens. Matter*, **18**, S1021–S1037.

Hundt, R., Schön, J. C., Hannemann, A. & Jansen, M. (1999). *J. Appl. Cryst.* **32**, 413–416.

Jang, J. H., Yoon, I. H. & Yoon, C. S. (2008). *Advanced Solid-State Photonics*, p. MC19. Washington: Optical Society of America.

Knyrim, J. S., Becker, P., Johrendt, D. & Huppertz, H. (2006). *Angew. Chem.* **118**, 8419–8421.

Le Bail, A., Duroy, H. & Fourquet, J. L. (1988). *Mater. Res. Bull.* **23**, 447–452.

Lennie, A. R., Laundy, D., Roberts, M. A. & Bushnell-Wye, G. (2007). *J. Synchrotron Rad.* **14**, 433–438.

Li, L., Li, G., Wang, Y., Liao, F. & Lin, J. (2005). *Inorg. Chem.* **44**, 8243–8248.

Mao, H. K., Xu, J. & Bell, P. M. (1982). *J. Geophys. Res.* **91**, 4673–4676.

Masood, G., Adolfo, E.-M. & Majid, E.-Z. (2006*a*). *Conference on Lasers and Electro-Optics/Quantum Electronics and Laser Science Conference and Photonic Applications Systems Technologies*, p. JThC64. Optical Society of America.

Masood, G., Adolfo, E.-M. & Majid, E.-Z. (2006*b*). *Conference on Lasers and Electro-Optics/Quantum Electronics and Laser Science Conference and Photonic Applications Systems Technologies*, p. JThC70. Optical Society of America.

Masood, G., Adolfo, E.-M. & Majid, E.-Z. (2007). *Conference on Lasers and Electro-Optics/Quantum Electronics and Laser Science Conference and Photonic Applications Systems Technologies*, p. JWA31. Optical Society of America.

Masood, G., Ivan, K., Andrzej, M., Edward, M. & Majid, E. (2004). *Conference on Lasers and Electro-Optics/International Quantum Electronics Conference and Photonic Applications Systems Technologies*, p. CThT37. Optical Society of America.

Masood, G. & Majid, E.-Z. (2005*a*). *Conference on Lasers and Electro-Optics/Quantum Electronics and Laser Science and Photonic Applications Systems Technologies*, p. CFL5. Optical Society of America.

Masood, G. & Majid, E.-Z. (2005*b*). *Conference on Lasers and Electro-Optics/Quantum Electronics and Laser Science and Photonic Applications Systems Technologies*, p. JTuC10. Optical Society of America.

Orosel, D., Balog, P., Liu, H., Qian, J. & Jansen, M. (2005). *J. Solid State Chem.* **178**, 2602–2607.

Orosel, D., Leynaud, O., Balog, P. & Jansen, M. (2004). *J. Solid State Chem.* **177**, 1631–1638.

Peltz, M., Bartschke, J., Borsutzky, A., Wallenstein, R., Vernay, S., Salva, T. & Rytz, D. (2005*a*). *Appl. Phys. B*, **80**, 55–60.

Peltz, M., Bartschke, J., Borsutzky, A., Wallenstein, R., Vernay, S., Salva, T. & Rytz, D. (2005*b*). *Appl. Phys. B*, **81**, 487–495.

Petrov, V., Noack, F., Tzankov, P., Ghotbi, M., Ebrahim-Zadeh, M., Nikolov, I. & Buchvarov, I. (2007). *Opt. Express* **15**, 556–563.

Rietveld, H. M. (1969). *J. Appl. Cryst.* **2**, 65–71.

Ruseva, V. & Hald, J. (2004). *Opt. Commun.* **236**, 219–223.

Shen, Y., Kumar, R. S., Pravica, M. & Nicol, M. F. (2004). *Rev. Sci. Instrum.* **75**, 4450–4454.

Spek, A. L. (2003). *J. Appl. Cryst.* **36**, 7–13.

Stein, W.-D., Cousson, A., Becker, P., Bohatý, L. & Braden, M. (2007). *Z. Kristallogr.* **222**, 680–689.

Sun, Z., Ghotbi, M. & Ebrahim-Zadeh, M. (2007). *Opt. Express* **15**, 4139–4148.

Sun, Z., Ghotbi, M., Minardi, S. & Ebrahim-Zadeh, M. (2007). *Conference on Lasers and Electro-Optics/Quantum Electronics and Laser Science Conference and Photonic Applications Systems Technologies*, p. CWB4. Optical Society of America.

Teng, B., Wang, J., Wang, Z., Jiang, H., Hu, X., Song, R., Liu, H., Liu, Y., Wei, J. & Shao, Z. (2001). *J. Cryst. Growth*, **224**, 280–283.
Tzankov, P. & Petrov, V. (2005). *Appl. Opt.* **44**, 6971–6985.
Umemura, N., Miyata, K. & Kato, K. (2007). *Opt. Mater.* **30**, 532–534.
Valentin, P., Frank, N., Pancho, T., Masood, G., Majid, E.-Z., Ivailo, N. & Ivan, B. (2007). *Conference on Lasers and Electro-Optics/Quantum Electronics and Laser Science Conference and Photonic Applications Systems Technologies*, p. CWB5. Optical Society of America.
Voigt, W. (1929). *Lehrbuch der Kristallphysik*. Leipzig: Teubner.